

Microcosm design and evaluation to study stream microbial biofilms

Gabriel Singer,¹ Katharina Besemer,¹ Iris Hödl,¹ Annkatrin Chlup,¹ Gerald Hochedlinger,¹ Peter Stadler,² and Tom J. Battin^{1,3}

¹Department of Freshwater Ecology, University of Vienna, Althanstr. 14, A-1090 Vienna, Austria

²Institute of Limnology, Austrian Academy of Sciences, Mondseestrasse 9, A-5310 Mondsee, Austria

³WasserCluster Lunz GmbH, Dr. Carl Kupelwieser Promenade 5, A-3293 Lunz am See, Austria

Abstract

Biofilms represent the dominant form of microbial life in stream ecosystems. Research of complex environmental biofilms requires appropriate cultivation techniques to address questions central to biofilm structure-function-coupling and ecosystem implications. Whereas the cultivation of medical and industrial biofilms has received considerable attention, cultivation devices for environmental biofilms have not. Here we describe and systematically assess the reproducibility of laboratory-based microcosms that allow the study of the structure and function of stream biofilms under different flow regimes. Microcosms were assembled from 1.3-m-long Plexiglas flumes fed with water that recirculated between a header tank and a sink. Each flume was paved with 104 individual unglazed ceramic coupons that served as growth substratum. We operated 3 microcosms designed to simulate laminar, transitional, and turbulent flow. Each microcosm consisted of two duplicate sets of flumes where two flumes shared the same water. We monitored biofilm coverage, bacterial abundance, and chlorophyll *a* as bulk biomass parameters over a growth period of 28 days and tested for community composition shifts using denaturing gradient gel electrophoresis (DGGE). Based on these variables, we assessed the reproducibility at different levels of microcosm assembly: (1) within individual flumes (i.e., longitudinal gradients), (2) within a shared water body, and (3) within flow regime treatments. Our results revealed good reproducibility at the various levels of the experimental setup and suggest microcosm flumes as highly valuable tools for biofilm studies with multitreatment and multireference designs.

Introduction

Biofilms are matrix-enclosed microbial accretions adhering to living and nonliving surfaces and represent a significant and incompletely understood mode of microbial growth (Costerton et al. 1995, Hall-Stoodley et al. 2004). For obvious reasons, most biofilm research has focused on detrimental and nuisance growth involved in infectious diseases and industrial processes during the last three decades (Costerton et al. 1999, Hall-Stoodley et al. 2004). By contrast, beneficial biofilm growth in natural environments has received significantly less attention despite the early research of stream biofilms (Geesey et al. 1978, Lock et al. 1984). This discrepancy is surprising given the functional relevance of microbial biofilms in natu-

ral environments and notably in sedimentary ecosystems such as streams (Lock et al. 1984, Battin et al. 2003).

Biofilm biology is complex and in general not well represented by flask cultures (Hall-Stoodley et al. 2004), nor is it fully understandable from in situ monitoring and semiexperimental observations in ecosystems as complex as streams (e.g., Battin et al. 2004, Romani et al. 2004). Mechanistic understanding of biofilm structure and function can be acquired only through carefully designed experiments under well-defined conditions. Therefore, model systems are required to simulate environmental conditions under different levels of experimental control.

Among the various laboratory-based experimental model systems developed, the flow chamber has become the gold standard for research on bacterial biofilm structure and function (e.g., Christensen et al. 1999, Palmer 1999, Heydorn et al. 2000, Venugopalan et al. 2005). Based on the conceptually simple parallel plate design (Bakker et al. 2003), these flow chambers allow direct and nondestructive biofilm growth and its on-line microscopic examination, and can be used in combination with various materials such as glass, silicone rubber, or dental enamel. These small-scale flow chambers, however,

*Corresponding author: Tom J. Battin¹ (tom.battin@univie.ac.at)

Acknowledgments

We are grateful to Bernhard Weinzinger for the technical drawing. This research was supported by Austrian Science Foundation grant P16935-B03 to T.J.B.

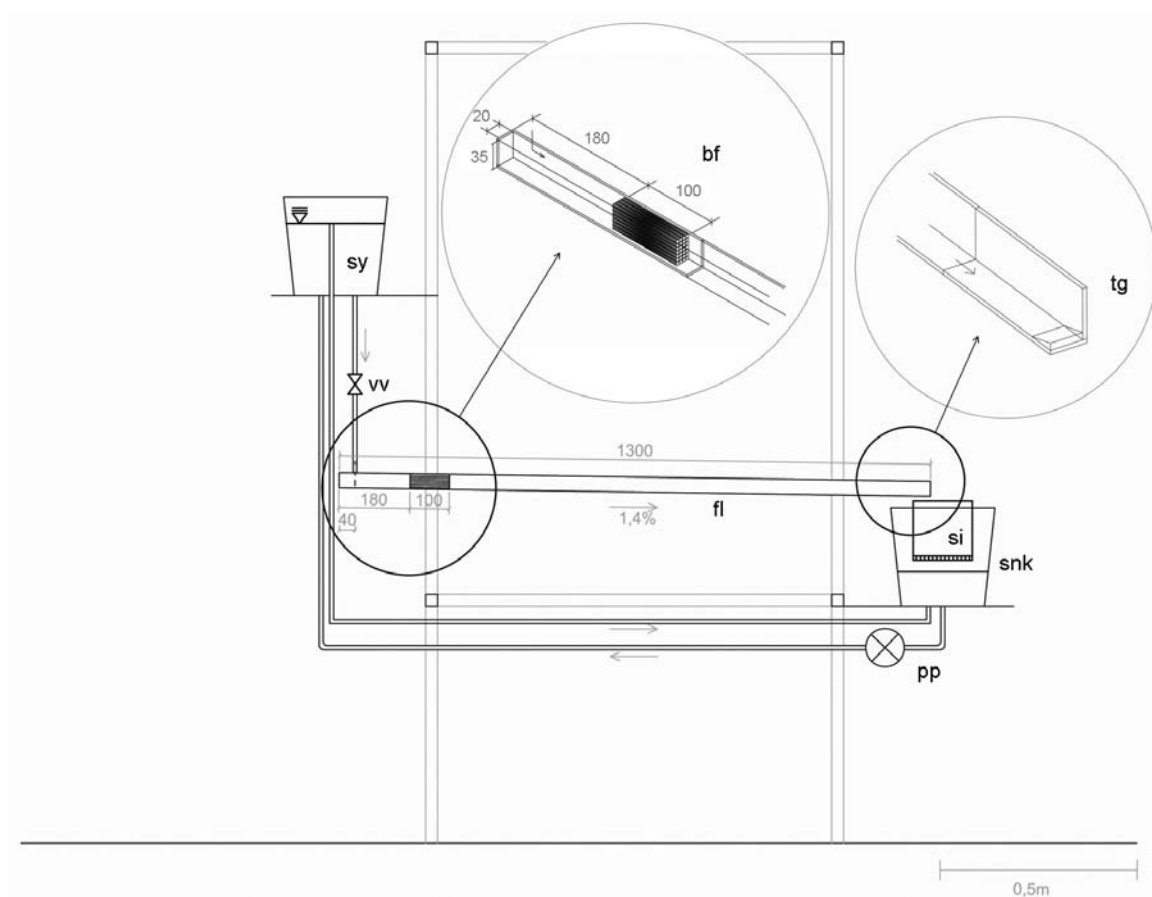


Fig. 1. Technical drawing of the flume setup (lateral view) and details of the baffle and tailgate construction (sy: siphon, snk: sink, vv: valve, si: sieve, fl: flume, tg: tailgate, bf: baffle, pp: pump).

are not well suited for the study of more complex biofilms from natural environments.

Rotating annular reactors and various bioreactors have been used to study structural features, effects of current velocity, metabolism, contaminant biodegradation, or sorption kinetics of microbial biofilms (e.g., Battin et al. 1999, Neu and Lawrence 1997, Lawrence et al. 2000, 2002, Pereira et al. 2002). These model systems are well suited to study biofilm structure and function in isolation, yet they do not effectively mimic the hydrodynamic and physicochemical conditions occurring in open channels and at the streambed interface. Flumes ranging from small-scale laboratory-based (Sabater et al. 2002, Mulholland et al. 1983) to large stream-side (Battin et al. 2003, Dodds and Biggs 2002) setups are highly suitable to study the coupling between hydrodynamics, chemistry, and microbial biofilm structure and function. Because of their large scale, flumes can also be used to study ecosystem implications of biofilms.

Because of the increasing use of laboratory-based flumes for environmental biofilm studies, it is essential to critically evaluate these setups. Reproducibility between and within microcosms is a necessary step toward successful sampling design and experiments—work that was done for small-scale flow cells (e.g., Heydorn et al. 2000), yet not for micro- and mesocosm flumes.

The aim of this study was to describe and systematically evaluate the reproducibility of flume microcosms designed to study hydrodynamic effects on stream biofilms. The hydrodynamic environment constitutes in fact a major physical template for biofilms in natural and engineered systems (Pereira et al. 2002, Battin et al. 2003, Venugopalan et al. 2005), and we therefore need reliable model systems. We cultivated stream biofilms in 12 replicate flumes with laminar, transitional, and turbulent flow regimes and tested reproducibility at multiple experimental levels. Bacterial abundance, chlorophyll *a*, and biofilm surface area coverage served as structural parameters measured on a large number of samples. Furthermore, community composition was analyzed on a selected set of samples using denaturing gradient gel electrophoresis (DGGE).

Materials and procedures

Flume design—Microcosms (Figures 1 and 2) consisted of flumes made of Plexiglas (length 1.3 m, width 0.02 m, height 0.02 m) with inlet baffles made from 5-cm-long tubes (diameter 5 mm) to smooth water flow. The flume outlet was open, and water freely drained into a sink to avoid changes in flow velocity due to backflow. Each flume was paved with 104 low-porosity, unglazed ceramic coupons (length 9.2 ± 0.3 mm,

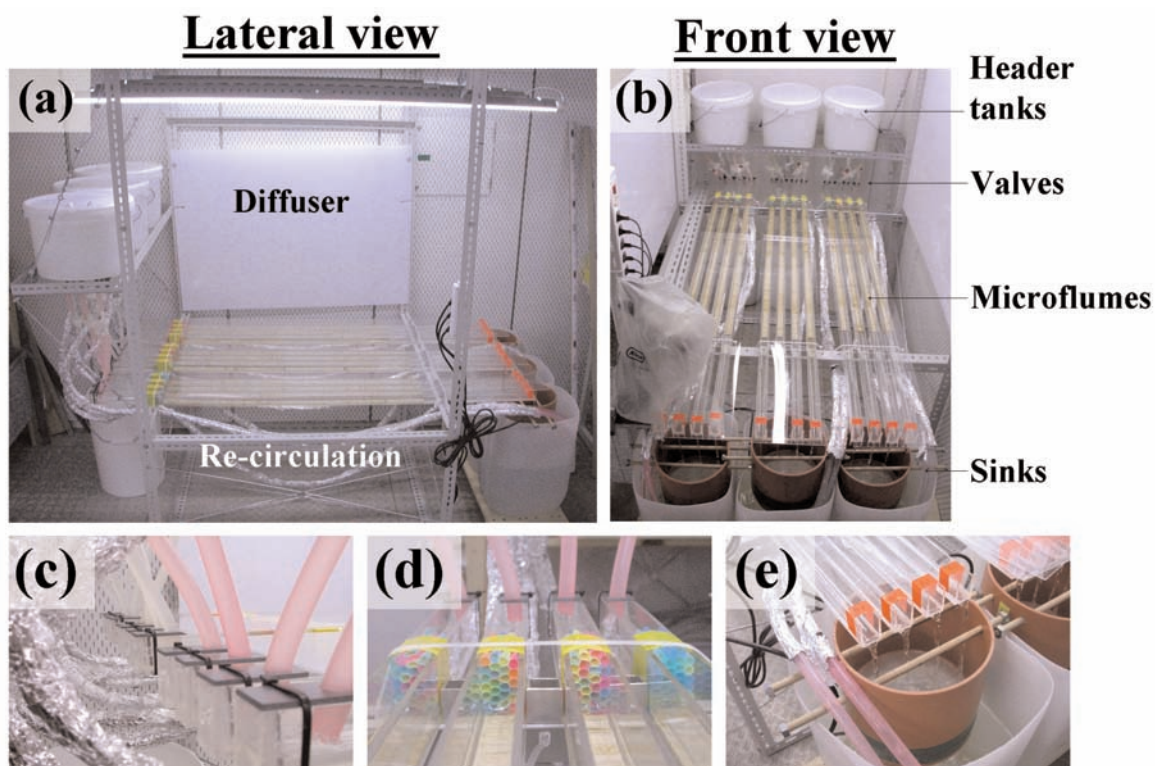


Fig. 2. Setup and components of the microcosm flumes. Lateral (a) and front (b) views, inlet (c), baffles (d), outlet and filter (e). (Pictures were taken during a different experiment with more flumes than described in the text and shown in Figure 3).

width 18.2 ± 0.3 mm, height 2.5 ± 0.15 mm) that served as substratum for biofilm growth. Coupons were made of natural clay (Westerwald, Germany) and baked at 1060°C to yield a porosity of approximately 10%. Several coupons at the beginning (6) and end (3) of the flume served as buffers to stabilize the hydrodynamic environment and were not used for sampling; no coupons were placed in the last 40 cm of the flume. An elastic silicon tube (diameter 2 mm) served as a spacer to prevent coupons from uplift and drift in the turbulent flow treatment; this was not necessary for the laminar and transitional treatments. Coupons were acid-washed twice (1 N HCl) to remove clay-bound inorganic nutrient ions, washed in deionized water, and finally combusted (450°C 4 h) to remove organic coatings. We assembled sets of 2 replicate flumes draining into one sink and fed with water by gravity from one header tank in a partially recirculating mode (Figures 1, 2, and 3). The header tank was continuously replenished from a pump submersed in the sink (submersible pump Aquamedic Ocean Runner 2500); 2 siphons (diameter 10 mm) directly draining from the header tank into the sink ensured constant head. All tubes were standard laboratory silicon tubes (inner diameter 10 to 14 mm). The total volume of recirculating water averaged 25 L for each set of duplicate flumes. Two sets of duplicate flumes (1 header tank and sink each) were assembled in each of the 3 flow treatments (Figure 3). This resulted in a total of 6 sets and 12 flumes. The 6 sets of duplicate flumes were fed from indi-

vidual water bodies throughout the experiment. Discharge was individually adjusted for each flume using a valve between the header tank and the flume inlet. Outlet water was continuously filtered through a $40\text{-}\mu\text{m}$ Nitex mesh to remove larger particles, sloughed biofilm fragments, and metazoan larvae.

Fluorescent tubes (58 W, TLD33 Philips) with reflectors yielded a mean photon flux density of $23.2 \mu\text{mol m}^{-2} \text{s}^{-1}$ within a range of $\pm 5 \mu\text{mol m}^{-2} \text{s}^{-1}$. Dark:light period was 12 h:12 h, and reflectors and lateral white diffusers minimized spatial heterogeneity of irradiance. Light distribution followed a flat unimodal distribution with a slight maximum above the center of the flume. Second-order polynomial regressions (minimum $R^2 > 0.9$) allowed the calculation of photon flux density above individual coupons. Microcosms were kept in an air-conditioned room at constant temperature of $20 \pm 1^\circ\text{C}$.

Hydrodynamic setting—Microcosms were designed to yield laminar, transitional, and turbulent flow treatments with initial parameters as described in Table 1. This was achieved by regulating flow rate and the slope of the flumes. Flow rate as the basic determining variable for the hydrodynamic environment was regularly checked throughout the experiment and adjusted within a 5% range if necessary. The dimensionless Reynolds number Re_f for open channel flow was calculated as

$$Re_f = u \frac{L_R}{\nu},$$

where u is current velocity, ν is kinematic viscosity, and L_R is

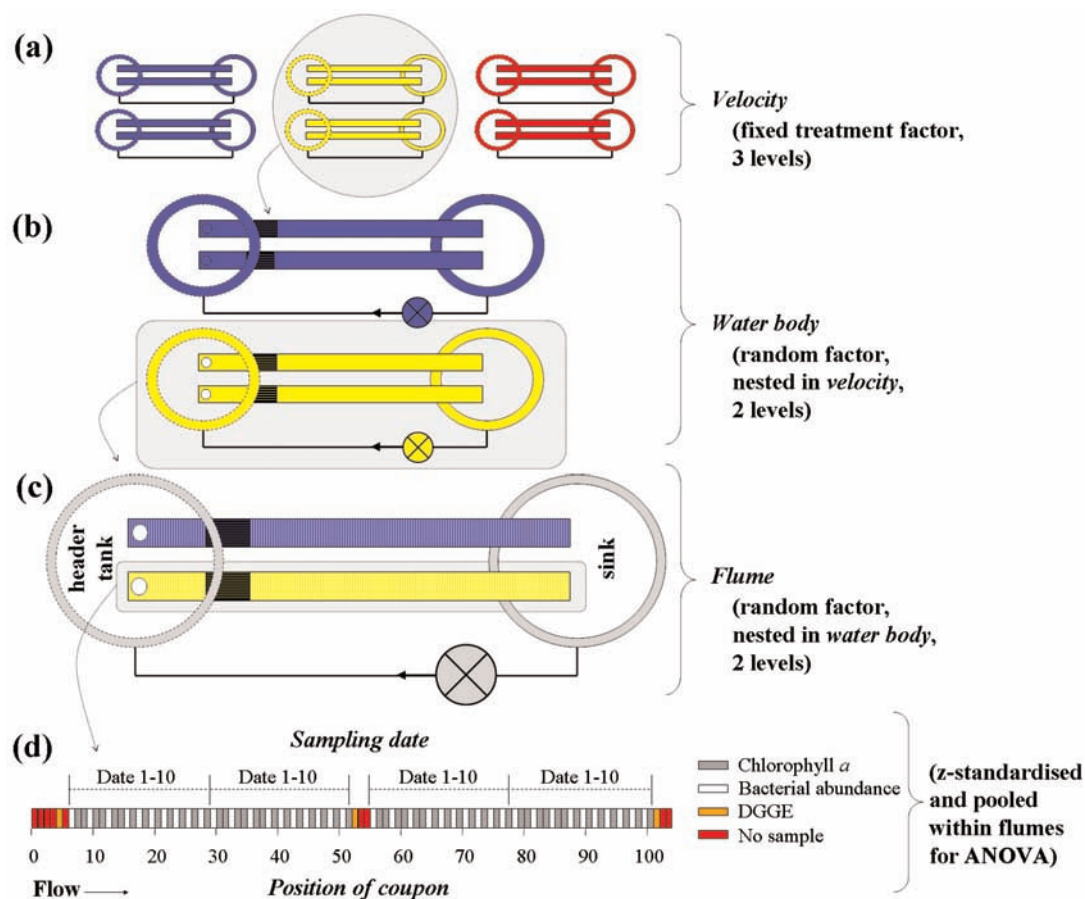


Fig. 3. Scheme of the sampling design for chlorophyll *a*, bacterial abundance, and DGGE showing various levels of replication. Factors of the mixed-model nested ANOVA were *velocity* (a), *water body* (b), and *flume* (c). Colors in (a), (b), and (c) denote different factor levels. Within 1 flume, coupons were collected on various positions and at different dates (d). After *z*-standardization per date, samples of 1 flume were pooled to yield an ANOVA error term with *df* = 39. Samples for DGGE were collected only once during the experiment.

the hydraulic radius calculated from the flume width (L_w) and water depth (L_h) according to

$$L_R = \frac{L_h L_w}{(L_w + 2L_h)}$$

The transition from laminar to transitional flow occurs at a Re_t value of about 500, and fully turbulent flow is typically associated with $Re_t > 2000$ (Dingman 1984). We injected rhodamine to visualize general flow patterns along the flumes in each flow treatment (Figure 4).

Stream water—Stream water originated from Weidlingbach, a fourth-order stream draining a largely forested catchment close to Vienna (Austria). Water was filtered through a 100- μ m mesh to remove major particles and insect larvae and transferred to the laboratory. Water recirculating in the flumes was

exchanged with new stream water every third day; 50% of the water was exchanged twice within 1 h, resulting in a total exchange of 75%. Nutrient concentrations in the new stream water averaged $2.13 \pm 4.63 \mu\text{g NH}_4\text{-N L}^{-1}$, $1055 \pm 160 \mu\text{g NO}_3\text{-N L}^{-1}$, and $5.50 \pm 1.37 \mu\text{g PO}_4\text{-P L}^{-1}$ (\pm standard deviation, $n = 16$); average conductivity was $459 \pm 54 \mu\text{S cm}^{-1}$, and average dissolved oxygen was $10.1 \pm 1.5 \text{ mg L}^{-1}$.

Sampling design—We grew microbial biofilms from raw stream water over a period of 28 days and collected samples for bacterial abundance and chlorophyll *a* every third day starting 12 h after the start of the microcosms. Each sample routinely consisted of 1 coupon retrieved from the flume with sterile forceps, but during initial growth (day 1 to day 5) we pooled duplicate coupons for chlorophyll *a* analysis. Based on

Table 1. Initial hydraulic characteristics of the 3 treatments.

Treatment	Flow rate, mL s^{-1}	Depth, cm	ν , cm s^{-1}	Re_t	Slope, %
Laminar	10	0.7	7.1	320	0.05
Transitional	25	0.7	18	798	0.4
Turbulent	60	0.7	43	1917	1.4

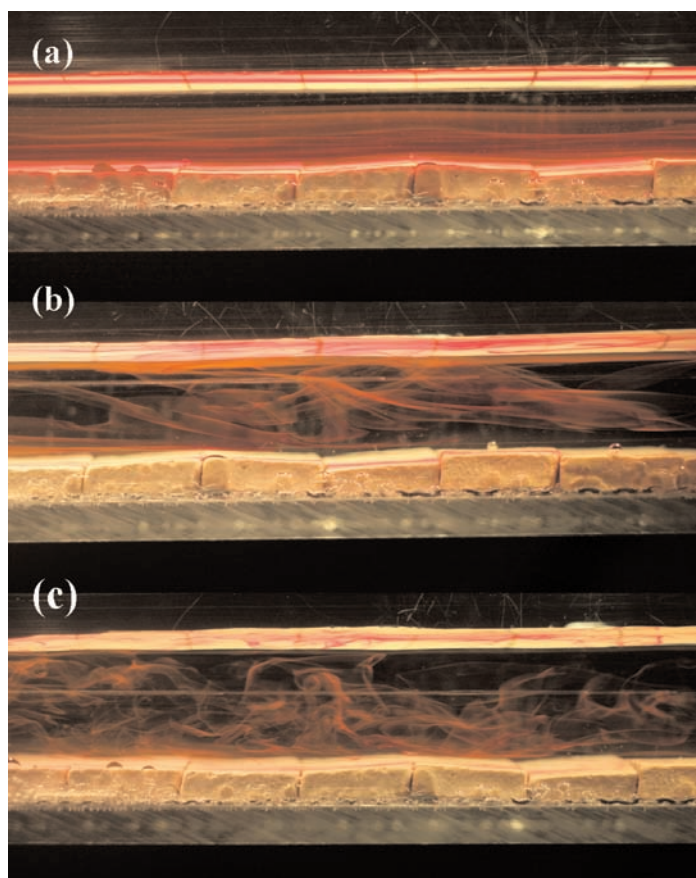


Fig. 4. Flow patterns in the laminar (a), transitional (b), and turbulent (c) flow treatments as visualized by rhodamine injections. Ceramic coupons are not colonized.

inspection with confocal laser scanning microscopy, biofilm growth on the sides of and underneath the coupons was negligible compared to the copious growth on surface exposed to water flow and light. Therefore, area-specific biomass always refers to the exposed surface area. To test for possible longitudinal gradients within flumes, samples for bacterial abundance and chlorophyll *a* were collected from 4 flume segments in each flume (Figure 3). To test for reproducibility within a set of duplicate flumes sharing the same body of water, and within the two sets of duplicate flumes of one flow treatment, we collected samples from corresponding positions in all 4 flumes of each treatment. Thus, all existing levels (treatment and random factors) of the experimental setup were sampled with extensive replication. This resulted in 480 individual samples each for bacterial abundance and chlorophyll *a*. Samples for DGGE were collected on day 18 during exponential growth as determined from bacterial abundance. We collected samples for DGGE from the upper, central, and lower part in each flume to test for longitudinal gradients and within-flow treatment reproducibility. This resulted in a total of 36 samples for DGGE. At each sampling date, sampled coupons were immediately replaced by sterile coupons to

avoid changing the hydrodynamic environment of the remaining coupons. At the end of the experiment (day 28), 240 of these replacement coupons were collected for the assessment of biofilm surface coverage as a basic structural variable. In each of 6 flumes, 4 replicate series of 10 coupons each were collected to test for reproducibility of biofilm surface coverage within flumes and within flow treatments. Within each flow treatment, we collected samples from two flumes belonging to separate sets of duplicate flumes. Due to the time-intensive nature of biofilm coverage analysis, replication at the flume level was omitted. Thus, biofilm surface coverage data could not be used to separately test for reproducibility between flumes of one set and between sets of flumes sharing the same water body.

Bacterial abundance—Samples were incubated with 0.1 mM tetrasodium pyrophosphate for 1 h and sonicated (180 s, 40 W output) to detach bacterial cells from the coupon (Velji and Albright 1986). Aliquots of the suspension were processed for flow cytometry using a FACScalibur flow cytometer (Becton Dickinson) equipped with an air-cooled laser providing 15 mW at 488 nm and standard filter setups (Gasol and Del Giorgio 2000). Before injection, samples were diluted (1:4 up to 1:40) with 0.2 μm filtered MilliQ water to achieve count rates ranging from 200 to 700 cells per second. Diluted samples were stained with 5 μM SYTO-13 (Molecular Probes) and kept at room temperature for at least 30 min (Del Giorgio et al. 1996).

Samples were automatically injected from Falcon tubes (10 mL) using a FACSauto loader (Becton Dickinson), which was set to mix samples (10 s) to avoid sedimentation of cells; this is very useful for standardized acquisition and analysis of flow cytometry samples. All parameters were collected with logarithmic amplification with trigger and threshold wavelengths set at 450 nm. Samples were counted at fixed flow rate, which was calibrated at the beginning and end of each analysis session using Truecount tubes (Becton Dickinson, cat. 340334); flow rate ranged either from 12 to 15 $\mu\text{L s}^{-1}$ at low speed or from 33 to 35 $\mu\text{L s}^{-1}$ at medium speed. Acquisition was achieved with CellQuest (Becton Dickinson) and analyses performed with Attractors.

Chlorophyll *a*—Chlorophyll *a* was extracted with *pro analysis* grade acetone during 12 h in the dark (4°C). Samples were thoroughly vortexed, and the supernatants were filtered (GF/F Whatman) and assayed fluorometrically (EX435/EM675) using spinach (Sigma-Aldrich) as standard.

Biofilm coverage—Standardized orthophotographs of biofilms (coupon scale, 1 by 2 cm) were taken with a Nikon F90 mounted on a Zeiss SMZ-1 stereomicroscope, digitized, and subjected to 3-channel (red, green, blue [RGB]) digital image analysis using the open source program ImageJ. The intensity frequency diagrams of the RGB channels (frequency distributions of 256 intensity values for each 8-bit-coded color channel) showed distinct patterns that allowed us to use the blue channel to distinguish between colonized (i.e., microbial biomass) and uncolonized coupon surface area. The uncolonized coupon

surface produced intensity values ranging from 255 to 40 in the blue channel. In contrast, coupon areas colonized with biofilm always produced intensity values below the threshold of 40. Optimal threshold identification was achieved by inspection of both uncolonized and fully colonized tiles and by visual calibration of selected pictures from the whole growth period. We therefore used the blue channel and an intensity threshold of 40 to calculate biofilm coverage (%) on a per-pixel basis.

DGGE—DNA was extracted from biofilms and purified with the UltraClean Soil DNA Isolation kit from MoBio (Carlsbad, CA, USA); uncolonized ceramic coupons served as negative controls. This extraction kit has been successfully used for environmental samples from different habitats (e.g., Besemer et al. 2005). Quantification and standardization of extracted DNA were achieved using a Fluorescent DNA Quantitation Kit (Bio-Rad Laboratories). Primers used for PCR were 341F (5'-CGC CCG CCG CGC CCC GCG CCC GGC CCG CCG CCC CCG CCC CCC TAC GGG AGG CAG CAG-3') and 907R (5'-CCG TCA ATT CCT TTG AGT TT-3') (Muyzer et al. 1993). Each 50- μ L PCR mixture contained 1 μ M of both primers (Thermo Electron GmbH, Germany), 0.25 mM each deoxynucleoside triphosphate, 2 mM MgCl₂, 50 μ g BSA, 1.25 U Taq polymerase, and the recommended PCR buffer (all from MBI Fermentas). Samples were amplified using the following protocol: an initial denaturation step of 94°C for 3 min, followed by 30 cycles of denaturation at 94°C for 40 s, annealing at 54°C for 40 s, and extension at 72°C for 1 min. Cycling was completed by a final extension at 72°C for 15 min. The PCR products were purified with the Qiaquick PCR Purification Kit (Qiagen), and their integrity was checked on 1% agarose gels (MBI Fermentas).

DGGE was performed using a DCode Universal Mutation Detection System (Bio-Rad) (Muyzer et al. 1993). PCR products were applied on 8% polyacrylamide gels (acrylamide:bisacrylamide 37.5:1) with gradients ranging from 30% to 70% (where 100% denaturant contains 7 M urea and 40% deionized formamide) and stacking gels on top (8% polyacrylamide, 0% denaturant). DGGE gels were run at constant voltage of 100 V at 60°C for 16 h in 1 \times TAE (pH 7.5). Gels were post-stained with Sybr Green I (Invitrogen), and bands were visualized with a UV transilluminator.

Statistical analyses—This article focuses on the reproducibility of the experimental setup rather than on the temporal aspects of biofilm growth itself. This approach allows a statistically more powerful consideration of reproducibility at various levels. For this purpose, bacterial abundance was log(x)-transformed, and chlorophyll *a* and biofilm surface coverage data were \sqrt{x} -transformed to fulfill conditions of normality and variance homogeneity for ANOVA. All data were then z -standardized within each sampling date according to:

$$z_{id} = \frac{x_{id} - \bar{x}_d}{s_d}$$

where the index *d* refers to the sampling date 1 to 10 and the index *i* refers to any value of a given sampling date. z -Standardization removes temporal variability from the primary

data. It thus greatly simplifies statistical analysis by reducing the factor number yet increasing the case number.

In our experimental design, random (i.e., uncontrolled) variation can occur at various experimental levels: (1) within flumes (i.e., variation between coupons), (2) between flumes sharing the same body of water (e.g., due to variation of hydrodynamics or light conditions), and (3) between water bodies (e.g., due to variation of water chemistry or inoculum). Using model II ANOVA, the total variance can be partitioned and various amounts of variation attributed to the various random factors (variance component analysis). Because our design included a treatment factor (model I ANOVA), we ran a 3-level mixed-model nested ANOVA (Figure 3) on z -standardized bacterial abundance and chlorophyll *a* with the factors *velocity* (fixed treatment, 3 levels), *water body* (random, nested in *velocity*, 2 levels), and *flume* (random, nested in *water body*, 2 levels) to test for effects of velocity or any random factor (general linear model tool in Statistica 5.5). A significant effect of a random factor, also termed a significant added variance component, indicates statistically important variation at this level of experimental design and necessary replication in future experiments (Sokal and Rohlf 1995). The random factor *water body* corresponds to a set of duplicate flumes sharing the same body of water (Figure 3). A similar analysis without distinguishing *water body* and *flume* as random factors was run for biofilm surface coverage as dependent variable.

Normality was tested using the Kolmogorov-Smirnov test on each factor level (individual flumes with $n = 40$ each) and for the entire data set after standardization per sample ($n = 480$) (Sokal and Rohlf 1995). Variance homogeneity was judged on Levene's test, Bartlett's chi-square test, and Hartley's F_{\max} test. The Moriguti-Bulmer procedure was used to calculate confidence limits of added variance components (Sokal and Rohlf 1995). The Tukey honest significant difference (HSD) test was employed for pairwise post-hoc comparisons between velocity treatments.

z -Standardized values of chlorophyll *a* and bacterial abundance were also used to test for existence of gradients within flumes by relating them to either coupon location or photon flux density as predictor variables in linear regressions. Photon flux density was calculated for each coupon location along individual flumes from polynomial regressions (see above). Regression analyses relating chlorophyll *a* or bacterial abundance to coupon location or photon flux density were run for each flume separately ($n = 40$), for each set of 2 flumes sharing the same body of water ($n = 80$), and for all data pooled within flow treatments ($n = 160$). In a similar analysis, we also pooled nonstandardized data from all flumes within each flow treatment and tested separately for each of the 10 sampling dates (i.e., 30 analyses with $n = 16$ each for each variable). We tested for linear relationships (1) because of the low variation of photon flux density (19.1 to 25.9 μ mol photons $m^{-2} s^{-1}$) in our systems and (2) because detection of unknown trends is most easily achieved by linear regression. Scatterplots were used to check for nonlinearity.

Table 2. Range and CV of chlorophyll *a*, bacterial abundance, and biofilm surface coverage during the 28-day experiment.

	Treatment		
	Laminar	Transitional	Turbulent
Chlorophyll <i>a</i> , $\mu\text{g cm}^{-2}$	0.007–5.51	0.004–4.90	0.001–3.03
CV, %	3.2–74.8	4.6–71.1	5.5–69.2
Bacterial abundance, 10^6 cells cm^{-2}	2.1–289.9	1.2–226.1	0.6–313.8
CV, %	5.5–46.3	7.5–53.8	5.4–69.9
Biofilm surface coverage, %	0.39–99.8	0.12–99.9	0.08–93.9
CV, %	2.5–121	1.4–92.2	1.4–86.7

Minimum and maximum values typically associated with the first and last sampling date, respectively. CV values were derived from data of single dates and single flumes.

We calculated the Sorensen coefficient as a dissimilarity index based on presence or absence of DGGE band data and subjected these values to nonmetric multidimensional scaling (MDS) analysis to segregate the various levels of variation (*velocity*, *water body*, *flume*) in community structure (Quinn and Keough 2002, Fromin et al. 2002). MDS was computed with Statistica 5.5 using principal components of the similarity matrix as the starting configuration for iterations under steepest descent followed by monotone regression transformation iterations (StatSoft 2001). The adequate number of dimensions to retain was judged from a scree plot (no. of dimensions vs. Kruskal's stress *S*).

Assessment

Our initial flume settings yielded hydrodynamic environments that are representative for conditions in high- to middle-

gradient streams. The coefficient of variation (CV) of the flow rate as the basic hydraulic variable was reasonably low, with 4.2%, 4.0%, and 3.6% for the laminar, transitional, and turbulent flow, respectively. This indicates generally good reproducibility within treatments. Constant width of rhodamine distribution in the flumes indicated stable flow starting approximately 5 cm downstream of the baffles. Rhodamine also visualized the laminar, transitional, and turbulent flow regimes (Figure 4).

Chlorophyll *a* concentrations ranged from 0.001 $\mu\text{g cm}^{-2}$ in the turbulent treatment (day 1) to 5.51 $\mu\text{g cm}^{-2}$ in the laminar treatment (day 28) (Table 2). Respective values for bacterial abundance were 0.6×10^6 cells cm^{-2} and 313.8×10^6 cells cm^{-2} (Table 2). Variability within individual flumes was relatively low; coefficients of variation within single dates and flumes ($n = 4$) averaged $26.5\% \pm 15.3\%$ and $23.0\% \pm 11.3\%$ (mean \pm SD) for chlorophyll *a* and bacterial abundance, respectively. The nested ANOVA approach allowed us to assign variation in chlorophyll *a* and bacterial abundance to the various levels of replication of the microcosms (Table 3, Figure 5). For both biomass variables, our analysis revealed most of the spatial variation occurring at the within-flume scale, as most variance was accounted for by the residual term (89%). This translates into good reproducibility at the levels of the random factors *flume* and *water body*. *Flume* as the next level of replication in the nested design produced a small but significant additional component of variance for both chlorophyll *a* (2.9%) and bacterial abundance (6.3%). *Water body* as the highest level of replication within the flow treatments did not produce a variance component significantly different from zero. *Velocity* as the fixed treatment significantly affected chlorophyll *a* and bacterial abundance.

Table 3. Results of mixed-model nested ANOVAs for chlorophyll *a*, bacterial abundance and biofilm surface coverage with *velocity* (fixed treatment), *water body* (random, nested in *velocity*), and *flume* (random, nested in *water body*) as factors.

Factor, source of variation	df1/df2	F	P	Variance component, %
Chlorophyll <i>a</i>				
<i>Velocity</i>	2/3	19.45	< 0.05	—
<i>Water body</i>	3/6	2.02	0.21	4.4 (–17.1, 115.5)
<i>Flume</i>	6/468	3.82	< 0.001	6.3 (1.3, 39.1)
Error	—	—	—	89.4
Bacterial abundance				
<i>Velocity</i>	2/3	13.86	< 0.05	—
<i>Water body</i>	3/6	4.41	0.06	8.7 (–3.2, 154.2)
<i>Flume</i>	6/468	2.32	< 0.05	2.9 (–0.1, 22.6)
Error	—	—	—	88.4
Biofilm surface coverage				
<i>Velocity</i>	2/3	28.86	< 0.05	—
<i>Flume/water body</i>	3/234	3.02	< 0.05	4.80 (–0.12, 97.5)
Error	—	—	—	95.2

For biofilm surface coverage, the random factors *flume* and *water body* cannot be distinguished because of sampling limitations. Confidence limits of added variance components were calculated by the Moriguti-Bulmer procedure.

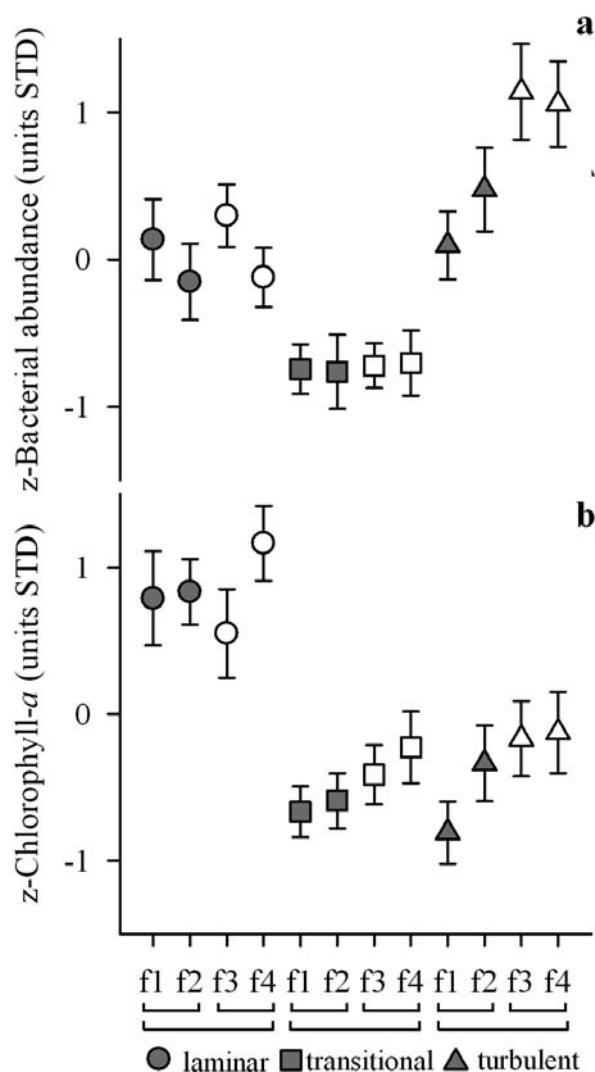


Fig. 5. Chlorophyll a (a) and bacterial abundance (b) in the 12 flumes, mean \pm 95% confidence limits of z -standardized data. Within each flow treatment, each set of 2 flumes (f1 and f2, f3 and f4) share the same body of water.

Biofilm surface coverage ranged from 0.08% in the turbulent treatment (day 1) to almost 100% in the transitional and laminar treatments (day 28). Again, variability within individual flumes was relatively low; coefficients of variation within single dates and flumes ($n = 4$) averaged $38.6\% \pm 30.8\%$ (mean \pm SD). The nested ANOVA approach clearly identified the residual term as the largest variance component (95.2%) and again revealed a small but significant variance component of the combined random factor *flume/water body* (4.8%). Because of the sampling design (no replication of flumes within water bodies), effects of *flume* and *water body* cannot be distinguished for this variable. Again a significant effect of the fixed treatment *velocity* was obvious.

The flume variance prompted us to further test for within flume gradients. z -Standardized chlorophyll a and bacterial abundance did not show any distinct linear or nonlinear

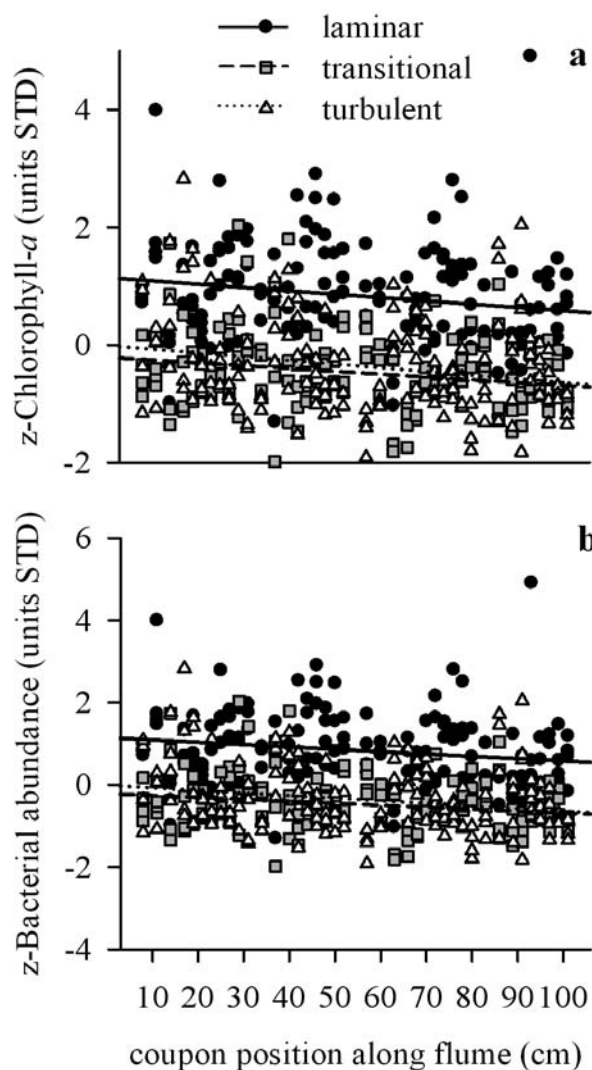


Fig. 6. Linear regressions of position of coupons in the flumes versus z -standardized chlorophyll a (a) and bacterial abundance (b) for the 3 flow treatments.

relationship with coupon location in the flume. When analyzed separately per flume ($n = 40$), no linear regression was significant except 3 analyses with low explanatory power ($r^2 = 0.12, 0.20, \text{ and } 0.30$). After data pooling within flow treatments, the large sample size ($n = 160$) produced significant relationships for chlorophyll a in all 3 treatments and a significant relationship for bacterial abundance in the laminar treatment (Figure 6, Table 4). However, explanatory power was extremely low ($r^2 < 0.1$) for all analyses (Table 4). Similarly, analyses of nonstandardized data performed separately for each sampling date were generally insignificant (26 of 30 separate analyses for chlorophyll a , 29 of 30 analyses for bacterial abundance).

Similar to coupon location, light distribution could not be identified as a significant predictor for chlorophyll a and bacterial abundance. Neither chlorophyll a nor bacterial abun-

Table 4. Results of linear regression analyses testing for gradients of chlorophyll *a* and bacterial abundance along the flumes.

Flow treatment	<i>P</i>	Slope	<i>R</i> ²
Chlorophyll <i>a</i>			
Laminar	< 0.05	-5.7×10^{-3}	0.032
Transitional	< 0.01	-4.8×10^{-3}	0.042
Turbulent	< 0.01	-6.3×10^{-3}	0.045
Bacterial abundance			
Laminar	0.68	8.9×10^{-4}	0.001
Transitional	< 0.01	-6.0×10^{-3}	0.071
Turbulent	0.20	-3.6×10^{-3}	0.010

Independent variable = coupon location; *n* = 160 for each analysis.

dance showed any distinct linear or nonlinear relationship with photon flux density when analyzed per flume (*n* = 40) or after pooling of data within flow treatments (*n* = 160). Any exceptional significant analyses showed extremely low explanatory power (maximum *r*² = 0.14). Again, analyses of nonstandardized data performed separately for each sampling date were generally insignificant (26 of 30 separate analyses for chlorophyll *a*, 30 of 30 analyses for bacterial abundance).

Analyses of DGGE gels identified a total of 26 distinct bands with a mean band number of 15 ± 2 per sample. The Sorensen dissimilarity index matrix based on presence or

absence of bands could be adequately represented by 2 dimensions in the MDS analysis; remaining Kruskal's standardized stress *S* was 0.067. The MDS analysis revealed 3 distinct clusters, which clearly corresponded to the 3 flow treatments (Figure 7). Between samples collected at the inlet, center, and outlet of flumes, variability was low and no meaningful patterns emerged, and they were therefore regarded as replicates within single flumes. Within-treatment reproducibility was good, and variability between water bodies was low (Figure 7). A 4-level mixed-model nested ANOVA similar to the analysis described above was run for the 2 dimensions of the MDS as response variables and the factors *velocity* (fixed treatment, 3 levels), *water body* (random, nested in *velocity*, 2 levels), and *flume* (random, nested in *water body*, 2 levels). For both MDS dimensions, only the factor *velocity* was significant (dimension 1: $F_{2,3} = 357$, $P < 0.001$, dimension 2: $F_{2,3} = 69.5$, $P < 0.01$).

Discussion

Controlled experiments with sufficiently large replication are essential for research on the effects of environmental factors on biofilm structure-function-coupling. The various flow chambers (Christensen et al. 1999) and rotating annular reactors (Lawrence et al. 2000) are certainly adequate to address questions related to microscale architecture. Flow chambers designed for online time-lapsed confocal imaging (e.g., Venu-

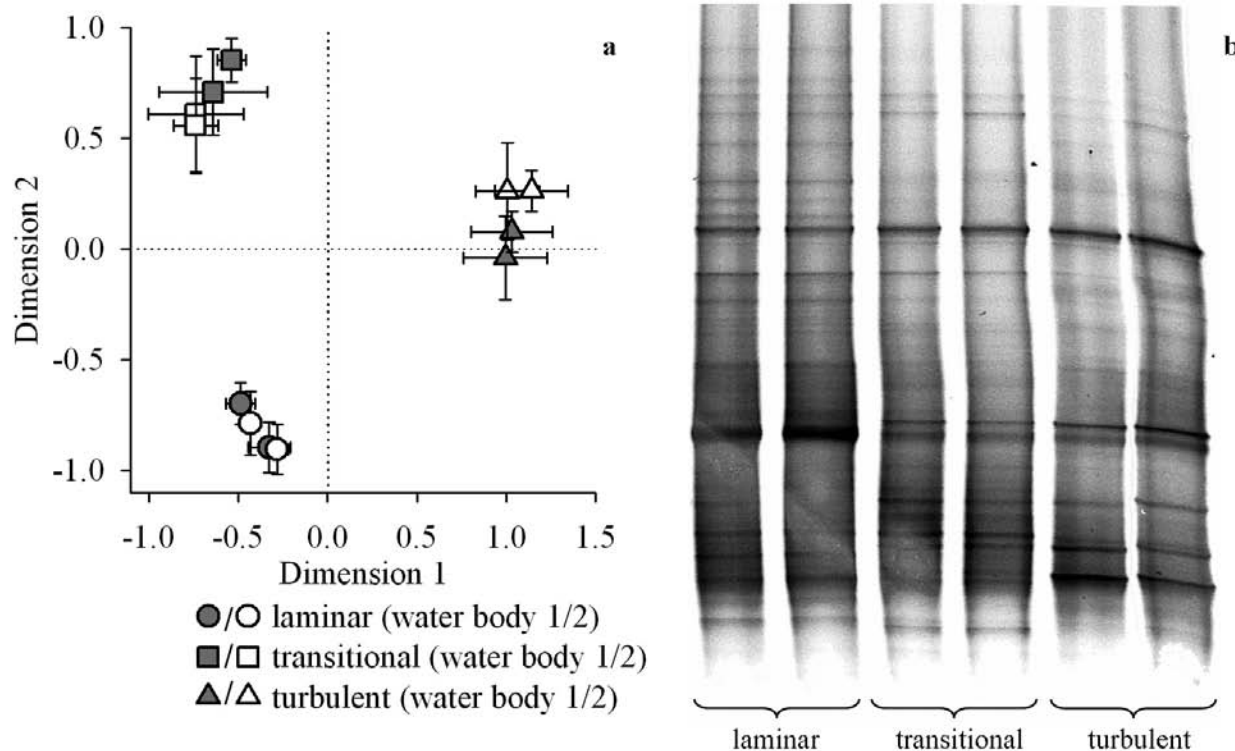


Fig. 7. (a) Multidimensional scaling of Sorensen dissimilarity indices between samples based on presence or absence of DGGE bands. Points represent means \pm SD of each flume (*n* = 3, samples collected at inlet, center, and outlet of flume). The graph shows relative similarity between flumes as distances in 2-dimensional space. (b) Representative DGGE gels of the 3 flow treatments.

gopalan et al. 2005), however, are typically small in scale (< 10 cm), and their hydrodynamic environment rarely reflects natural conditions. Rotating annular reactors, on the other hand, are characterized by mixing and transport processes that are not truly representative of the physical environment experienced by microbial biofilms in stream ecosystems. Flumes as described and assessed in this article and used by others (e.g., Sabater et al. 2002) serve the demands of stream microbial ecologists interested in the coupled physical, chemical, and biological processes (Packman et al. 2003) operating at the streambed interface.

As outlined by Gjaltema and Griebe (1995) and further developed by Lawrence et al. (2000), the reactor design for biofilm cultivation should consider hydrodynamic mixing, substrate supply, development of gradients, accessibility for sampling, monitoring of growth, septic operation, nature of substratum, and maintenance of community composition and structure (i.e., architecture). These parameter settings should result in a well-defined environment as a prerequisite to cultivate defined biofilm communities through natural selection and involving primary colonization, gradual succession, and subsequent formation of a dynamic climax community (Caldwell 1995).

Our flumes fulfilled these considerations. As shown by the reasonably low coefficients of variation of flow rate but also by flow patterns emerging from the rhodamine injections, microcosms had reproducible hydrodynamic environments. Furthermore, continuous and fast turnover of water within the various subsystems of relatively high water volume (i.e., 0.3 L of a single flume volume vs. almost 25 L of the total system) result in a well-defined environment in terms of hydrodynamics and mass fluxes. Our analyses covered various levels of biofilm organization and ranged from the relative biofilm surface area coverage to bacterial abundance, chlorophyll *a*, and DGGE fingerprints. No variable showed a detectable gradient within flumes, suggesting that both flume geometry and inlet and outlet conditions generate stable and uniform flow within a reasonably long part of the flume length (cf Bakker et al. 2003). Patterns of rhodamine development along the flow path support this observation. Variability within individual flumes was relatively low for all variables, indicating minimal spatial variability of biofilm structure within the same flume. Furthermore, all variables demonstrated very good reproducibility at the higher levels of experimental replication (i.e., among water bodies and among flumes). The mixed-model nested ANOVAs run for chlorophyll *a*, bacterial abundance, and coverage identified a small but significant variance component of the random factor *flume* in addition to the variance existing within individual flumes, which indicates necessary replication at the level of flumes. The identification of reproducibility of biofilm structure at the various levels of experimental design is a basic requirement for successful experimental work with reference and multiple treatment flumes, especially for system-level measurements (e.g., biofilm growth and particle or contaminant transport). Our assessment suggests that effort should be

allocated to sampling between and within flumes, while sets of flumes sharing the same water bodies (i.e., header tank) can be used for multitreatment designs (e.g., differing water chemistry or inocula). The effects of flow regime on biofilm structure will be discussed elsewhere (K. Besemer, I. Hödl, G. Singer and T. J. Battin, unpublished results).

Unglazed ceramic coupons served as substrata for biofilm growth in our flumes, whereas others used glass slides or polycarbonate coupons (e.g., Lawrence et al. 2000, Venugopalan et al. 2005). Both texture and geochemistry of ceramic coupons are closer to the properties of natural sedimentary substrates, and the resulting biomass values were comparable to those from streams (Battin et al. 2004). Heterogeneity is inherent to both mono- and multispecies biofilms (Hall-Stoodley et al. 2004, Venugopalan et al. 2005), and therefore a sufficiently high number of samples with sufficiently large surface areas is required. Each of our flumes was packed with 104 reproducible individual coupons large enough to detect selected variables and allowing for extensive sampling. Their large total surface area should also ensure measurements of mass retention at the microcosm scale.

Comments and recommendations

Experiments running over a prolonged time (> 3 weeks) with high total radiation and algal inoculum require systematic and careful maintenance of the microcosms. Substantial growth of algae in the header tanks and various tubing systems can reduce flow rate through fouling, or retain particles, and solutes and thereby introduce an error term in mass balance experiments. These system components must therefore be regularly cleaned. Gently massaging silicone tubes works fine to inhibit biofouling and clogging of the tubing system; larger surfaces in header tanks or sinks may be scraped and detached biomass can easily be removed. The online sieves (40 μm) are useful to remove particles and sloughed biofilm fragments from the flume effluents and to prevent extended recirculation of this potentially erosive material. If required, sieving may also be useful to prevent growth of grazers introduced with raw stream water. Tubing systems should be wrapped with aluminum foil to minimize algal growth.

Flow rate is the major factor driving the hydrodynamic environment in the flumes and therefore deserves careful attention. It should be checked on a daily basis and valves adjusted accordingly. Online readings of flow rate using automated or semiautomated devices would greatly facilitate this task. Baffles are crucial to achieve stable flow within a distance as short as possible to maximize surface areas available for colonization. Baffles should be carefully scaled to the flume dimensions and flow rate. This can easily be achieved empirically with dye injections.

Our flumes did not have tailgates to adjust the water energy line, and we therefore observed nonuniform flow (i.e., slightly decreasing water depth) within the last 20 to 30 cm of the flumes. This drop depends of course on the slope set for each

flume system. Although we did not collect any samples in this area of nonuniform flow and could not detect any biomass gradients within the remaining area of the flume, we will implement miniature tailgates to produce uniform flow over the entire flume length for future work. Tailgates typically consist of a small ramp mounted at the end of the flume (Figure 1); their dimensions must be scaled exactly to the flume discharge and slope to produce uniform flow (i.e., constant water depth). This will also be important for mass balance approaches at the scale of the whole flume, as depth affects mass transfer.

A major advantage of the flumes is the accessibility and universal usability of the coupons for various analyses. However, removed coupons should be replaced immediately by sterile coupons to avoid wake interference and skimming flow. Scale and accessibility of the described experimental setup also allows individual flumes to be easily equipped with microscopes, high-resolution digital cameras, and other online monitoring devices. Finally, microcosms can easily be disinfected by recirculating sodium hypochloride (1.2%) through all system components.

References

- Bakker, D. P., A. van der Plaats, G. J. Verkerke, H. J. Busscher, and H. C. van der Mei. 2003. Comparison of velocity profiles for different flow chamber designs used in studies of microbial adhesion to surfaces. *Appl. Environ. Microbiol.* 69:6280-6287.
- Battin, T. J., A. Butturini, and F. Sabater. 1999. Immobilization and metabolism of dissolved organic carbon by natural sediment biofilms in a Mediterranean and temperate stream. *Aq. Microb. Ecol.* 19:297-305.
- , L. A. Kaplan, J. D. Newbold, and C. M. E. Hansen. 2003. Contributions of microbial biofilms to ecosystem processes in stream mesocosms. *Nature* 426:439-442.
- , A. Wille, R. Psenner, and A. Richter. 2004. Large-scale environmental controls on microbial biofilms in high-alpine streams. *Biogeosciences* 1:159-171.
- Besemer, K., M. M. Moeseneder, J. M. Arrieta, G. J. Herndl, and P. Peduzzi. 2005. Complexity of bacterial communities in a river-floodplain system (Danube, Austria). *Appl. Environ. Microbiol.* 71:609-620.
- Caldwell, D. E. 1995. Cultivation and study of biofilm communities. In H. M. Lappin-Scott and J. W. Costerton [eds.] *Microbial Biofilms*. University Press, Cambridge, UK, p. 64-79.
- Christensen, B. B., and others. 1999. Molecular tools for study of biofilm physiology. *Methods Enzymol.* 310:20-42.
- Costerton, J. W., Z. Lewandowski, D. E. Caldwell, D. R. Korber, and H. M. Lappin-Scott. 1995. Microbial biofilms. *Annu. Rev. Microbiol.* 49:711-745.
- , P. S. Stewart, and E. P. Greenberg. 1999. Bacterial biofilms: a common cause of persistent infections. *Science* 284:1318-1322.
- Del Giorgio, P. A., D. F. Bird, Y. T. Prairie, and D. Planas. 1996. Flow cytometric determination of bacterial abundance in lake plankton with the green nucleic acid stain SYTO 13. *Limnol. Oceanogr.* 41:783-789.
- Dingman, S. L. 1984. *Fluvial Hydrology*. Freeman and Company, New York.
- Dodds, W. K., and B. J. F. Biggs. 2002. Water velocity attenuation by stream periphyton and macrophytes in relation to growth form and architecture. *J. N. Am. Benthol. Soc.* 21:2-15.
- Fromin, N., and others. 2002. Statistical analyses of denaturing gel electrophoresis (DGE) fingerprinting patterns. *Environ. Microbiol.* 4:634-643.
- Gasol, J. M., and P. A. Del Giorgio. 2000. Using flow cytometry for counting natural planktonic bacteria and understanding the structure of planktonic bacterial communities. *Sci. Mar.* 64:197-224.
- Geesey, G. G., J. W. Mutch, J. W. Costerton, and R. B. Green. 1978. Sessile bacteria: an important component of the microbial population in small mountain streams. *Limnol. Oceanogr.* 23:1214-1223.
- Gjaltema, A., and T. Griebe. 1995. Laboratory biofilm reactors and on-line monitoring. *Water Sci. Technol.* 32:257-261.
- Hall-Stoodley, L., J. W. Costerton, and P. Stoodley. 2004. Bacterial biofilms: from the natural environment to infectious diseases. *Nat. Rev. Microbiol.* 2:95-108.
- Heydorn, A., B. K. Ersbøll, M. Hentzer, M. R. Parsek, M. Givskov, and S. Molin. 2000. Experimental reproducibility in flow-chamber biofilms. *Microbiology* 146:2409-2415.
- Lawrence, J. R., A. B. Scharf, B. G. Packroff, and T. R. Neu. 2002. Microscale evaluation of the effects of grazing by invertebrates with contrasting feeding modes on river biofilm architecture and composition. *Microb. Ecol.* 44:100-207.
- , G. D. W. Swerhone, and T. R. Neu. 2000. A simple rotating annular reactor for replicated biofilm studies. *J. Microbiol. Methods* 42:215-224.
- Lock, M. A., R. R. Wallace, J. W. Costerton, R. M. Ventullo, and S. E. Charlton. 1984. River epilithon: toward a structural-functional model. *Oikos* 42:10-22.
- Mulholland, P. J., J. D. Newbold, J. W. Elwood, and C. L. Hom. 1983. The effect of grazing intensity on phosphorus spiralling in autotrophic streams. *Oecologia* 58:358-366.
- Muyzer, G., E. C. DeWaal, and A. G. Uitterlinden. 1993. Profiling of complex microbial populations by denaturing gradient gel electrophoresis analysis of polymerase chain reaction-amplified genes coding for 16S rRNA. *Appl. Environ. Microbiol.* 59:695-700.
- Neu, T. R., and J. R. Lawrence. 1997. Development and structure of microbial biofilms in river water studied by confocal laser scanning microscopy. *FEMS Microb. Ecol.* 24:11-25.
- Packman, A. I., T. J. Battin, and D. J. Newbold. 2003. Coupling of hydrodynamical, biological, and geochemical processes in streambeds. *Arch. Hydro-Engineer. Environ. Mech.* 50:107-123.
- Palmer, J. R. Jr. 1999. Microscopy flowcells: perfusion chambers for real-time study of biofilms. *Methods Enzymol.* 310:160-166.
- Pereira, M. O., M. Kuehn, S. Wuertz, T. Neu, and L. F. Melo. 2002. Effect of flow regime on the architecture of *Pseudomonas fluorescens* biofilm. *Trends Microbiol.* 78:164-171.

- Quinn, G. P., and M. J. Keough. 2002. *Experimental Design and Data Analysis for Biologists*. Cambridge University Press, Cambridge, UK.
- Romani, A. M., A. Giorgi, V. Acuna, and Sabater S. 2004. The influence of substratum type and nutrient supply on biofilm organic matter utilization in streams. *Limnol. Oceanogr.* 49: 1713-1721.
- Sabater, S., E. Navarro, and H. Guas. 2002. Effects of copper on algal communities at different current velocities. *J. Appl. Phycol.* 14:391-398.
- Sokal, R. R., and F. J. Rohlf. 1995. *Biometry: The Principles and Practice of Statistics in Biological Research*. Freeman & Co., New York.
- StatSoft, Inc. 2001. Statistica (data analysis software system), version 5.5 www.statsoft.com.
- Velji, M. J., and L. J. Albright. 1986. Microscopic enumeration of attached marine bacteria of seawater, marine sediment, fecal matter, and kelp blade samples following pyrophosphate and ultrasound treatment. *Can. J. Microbiol.* 32:121-126.
- Venugopalan, V. P., M. Kuehn, D. Springael, P. A. Wilderer, and S. Wuertz. 2005. Architecture of a nascent *Sphingomonas* sp. biofilm under varied hydrodynamic conditions. *Appl. Envir. Microbiol.* 71:2677-2686.

Submitted 17 February 2006

Revised 11 July 2006

Accepted 22 August 2006